DOI 10.48612/fpg/zkvg-71uu-xk44

The Institute of Computational Mathematics and Mathematical Geophysics SB RAS; 6, Ac. Lavrentieva ave., Novosibirsk, 630090, Russia
*E-mail: iakshina.dina@gmail.com

RECENT CLIMATIC CHANGE RESEARCH IN THE CHUKCHI AND BEAUFORT SEAS BASED ON NUMERICAL SIMULATION

Received 12.01.2022, Revised 12.04.2022, Accepted 06.05.2022

Abstract

This study analyses climatic changes in the Chukchi Sea and the Beaufort Sea based on numerical modeling using a regional ice-ocean model. Numerical experiments were carried out for the period 2000–2019. NCEP/NCAR reanalysis data were used to determine the ocean and sea ice surface fluxes. The temperature, salinity, and transport of Pacific waters entering the Arctic Ocean were specified as boundary conditions in the Bering Strait. Three types of boundary values were used for the experiments: a) monthly average climate data averaged over the period 1990–2004; b) monthly average climate data averaged over the period 2003–2015; c) average monthly measurement data since 2016 to 2019. The sensitivity of the model to the variability of the transport and temperature of the incoming Pacific waters was studied, and the effect on the ocean heat content, the volume and sea ice extent were analyzed.

Numerical experiments simulate the transport of warm Pacific water across the Chukchi shelf in the north direction and onto the Beaufort Sea shelf, the process of warm water sinking on the continental slope in the autumn-winter period. In recent years, at the points on the boundary of the shelf and deep-water areas, the amplitude of seasonal temperature fluctuations in the surface layer increases and the temperature rises significantly at a depth of 100 m.

The simulation results demonstrate an increase in the ocean heat content and decrease in the ice volume in the Beaufort and Chukchi Seas, caused by an increase in atmospheric temperature. We also showed that the increase in temperature and transport of the Pacific water, which began after 2003, contributed to an additional increase in the ocean heat content of both seas, a reduction in the ice cover area, and a delay in the ice formation in the Chukchi Sea.

Keywords: climate change, numerical modeling, sea ice, Arctic Ocean, ocean-ice numerical model, Chukchi Sea, Beaufort Sea, Bering Strait

Институт вычислительной математики и математической геофизики Сибирского отделения РАН; пр. Академика Лаврентьева, д. 6, 630090, г. Новосибирск, Россия
*E-mail: iakshina.dina@gmail.com

ИССЛЕДОВАНИЕ КЛИМАТИЧЕСКИХ ИЗМЕНЕНИЙ В ЧУКОТСКОМ МОРЕ И МОРЕ БОФОРТА НА ОСНОВЕ ЧИСЛЕННОГО МОДЕЛИРОВАНИЯ

Статья поступила в редакцию 12.01.2022, после доработки 12.04.2022, принята в печать 06.05.2022

Аннотация

На основе численного моделирования с использованием региональной модели океана и морского льда исследуются климатические изменения в Чукотском море и море Бофорта. Численные эксперименты проводились для временного периода 2000–2019 гг. Данные реанализа атмосферы NCEP/NCAR использовались для определения потоков на поверхности океана и морского льда. Температура, соленость и расход тихоокеанских вод, поступающих в Северный Ледовитый океан, задавались в виде граничных условий на Беринговом проливе. Для проведения экспериментов использовались три типа граничных значений: среднемесячные климатические данные, характерные для 1990–2004 и 2003–2015 гг.; среднемесячные данные измерений в период 2016–2019 гг. Исследовалась чувствительность модели к изменчивости расхода и температуры поступающих тихоокеанских вод, анализировалось влияние на теплосодержание верхнего слоя моря, объем и распределение ледового покрова.

Ссылка для цитирования: *Якшина Д.Ф.*, *Голубева Е.Н.* Исследование климатических изменений в Чукотском море и море Бофорта на основе численного моделирования // Фундаментальная и прикладная гидрофизика. 2022. Т. 15, № 2. С. 60–75. doi:10.48612/fpg/zkvg-71uu-xk44
For citation: *Iakshina D.F.*, *Golubeva E.N.* Recent Climatic Change Research in the Chukchi and Beaufort Seas based on numerical simulation. *Fundamental and Applied Hydrophysics*. 2022, 15, 2, 60–75. doi:10.48612/fpg/zkvg-71uu-xk44

В численных экспериментах моделируется перенос теплых тихоокеанских вод через Чукотский шельф в северном направлении и на шельф моря Бофорта, процесс переноса теплых вод склоновой конвекцией в осенне-зимний период. В последние годы расчета в точках на границе шельфовой и глубоководной областей происходит увеличение амплитуды сезонных колебаний температуры поверхностного слоя и значительное повышение температуры на глубине 100 м. Результаты расчетов демонстрируют увеличение теплосодержания вод и сокращение объема льда в море Бофорта и Чукотском море, вызванное повышением температуры атмосферы. Показано, что повышение температуры и расхода тихоокеанских вод, начавшееся после 2003 года, способствовало дополнительному повышению теплосодержания вод обоих морей, сокращению площади ледового покрова и задержке сроков формирования льда в Чукотском море.

Ключевые слова: климатические изменения, численное моделирование, морской лед, Северный Ледовитый океан, региональная модель океана и морского льда, Чукотское море, море Бофорта, Берингов пролив

1. Introduction

One of the main physical mechanisms that shape the state of the hydrological regime of the Arctic Ocean is its interaction with the waters of the Atlantic and Pacific oceans [1]. Pacific waters enter the Arctic Ocean through the relatively narrow (~85 km) and shallow (~50 m) Bering Strait due to the level difference between the oceans [2–4]. Pacific waters are one of the sources of heat, fresh water [5], and nutrients [6] for the Arctic Ocean.

Passing through the shelf of the Chukchi Sea as a surface current, Pacific waters warm up in summer and are also transformed due to exchange with the atmosphere and mixing processes with shelf waters. Spreading further north, they sink because they have higher salinity than ocean surface water. Then they are propagated by the system of currents in the deep part of the basin in a layer of 50–150 m [7], giving off heat to adjacent layers and contributing to an increase in the temperature of the surface layer. Cold Winter Pacific waters maintain the state of a cold Arctic halocline [8].

Observation data show that the transfer of Pacific waters to the deep part of the Arctic basin is carried out by currents. The trajectory of the currents is influenced by ice conditions, wind impact, and bottom topography [9]. It follows from [10] that the anticyclonic gyre of the Beaufort Sea and the generation of mesoscale eddies in the areas of submarine canyons weaken the cyclonic boundary current and contribute to the movement of Pacific waters into the inner halocline of the Canadian Basin. Mesoscale eddies on the continental slope of the Beaufort Sea [11, 12] play a significant role in this. In addition, the work [13] showed that where Pacific waters are on the surface, Ekman convergence can lead to water subduction and subsequent transfer in the Beaufort Gyre. A detailed discussion of a possible mechanism for the transport of Pacific waters to the deep Arctic is included in the work [14].

The heat transported by the waters coming through the Bering Strait has the most significant effect on the seasonal melting of sea ice in the Chukchi Sea area [15, 16]. The work [17] showed that the date of retreat of the ice cover in the Chukchi Sea correlates by 80 % with the influx of heat into the Bering Strait from April to June. The volume of Pacific water entering the Arctic through the Bering Strait is 0.8–1.2 Sv (1 Sv = 10^6 m^3/s) with a heat content of 12 TW. [18]. The works [18, 19] showed, based on the analysis of observational data that in recent decades, the water transport increased by ~0.01 Sv/year from 1990 to 2019, which had an impact on the thermohaline structure of the Chukchi Sea and contributed to the intensification of sea ice melting [17]. The work [20] shows that in one of the main structures of the Arctic Basin, the Beaufort Gyre, over the past three decades (1987–2017), the heat content (relative to the freezing point) of the halocline has almost doubled. The warming of the halocline is associated by the authors of the work with anomalous solar heating of surface waters in the north of the Chukchi Sea, where the absorption of solar heat in summer increased five times [20], mainly due to the disappearance of the ice cover. Estimates of the solar heat accumulated by surface waters and the rate of sinking of these waters are consistent with the observed warming of the halocline. The authors of the paper ask whether a possible further increase in heat absorption on the shelf of the Chukchi Sea will affect the increase in heat content and the rate of growth and melting of ice in the Beaufort Sea.

In this paper, based on a three-dimensional numerical model of the ocean and sea ice, we study the sensitivity of the oceanic and ice characteristics of the Chukchi and Beaufort Seas to an increase in temperature and intensity of the inflow of Pacific waters. The process of heat transfer, which is formed in the bottom layers of the Chukchi shelf, along the continental slope is modeled. The temporal variability of ice volume and heat content in the Beaufort and Chukchi Seas is analyzed as a response to changes in the characteristics of Pacific waters in the Bering Strait.

2. Materials and methods

2.1. Numerical model

The numerical ocean-ice model SIBCIOM (Siberian Coupled Ice-Ocean Model) developed at ICMMG SB RAS was used for the study. The oceanic part is presented in detail in [21, 22]. The equations representing the laws of conservation of heat, salt, and momentum are written in an orthogonal curvilinear coordinate system and a physical z-vertical coordinate system using the Boussinesq and hydrostatic approximations. Numerical algorithms involve the use of explicit and semi-implicit schemes. The numerical scheme for the transfer operators is based on the third-order scheme QUICKEST [23] and its multidimensional implementation COSMIC [24]. When carrying out numerical experiments, the diffusion coefficients in the heat and salt transfer equations were equal to zero, which left only scheme diffusion in the model.

Some physical processes that are not described within the framework of the grid resolution of the model are included as parameterizations, in particular, the parametrizations of vertical convective and turbulent mixing [25] and slope convection [26] are used.

The elastic-viscous-plastic model of sea ice CICE-3 is used as an ice block [27].

For numerical experiments, the area of the Arctic Ocean and the northern and equatorial parts of the Atlantic Ocean are considered, starting from 20° S. For the numerical approximation of the equations, a tripolar grid is used [28]. The nodes of the numerical grid in the Arctic Ocean are at a distance of 10–25 km. The vertical subdivision consists of 38 horizontal levels with a concentration near the surface, where the resolution is 2.5 m. The most significant straits within the Canadian archipelago are included in the modeling area. The minimum depth of the shelf zone is set to 12.5 m.

On the "solid" lateral boundaries, the no-slip conditions for the velocity and the conditions for the absence of heat and salt fluxes were set. The "liquid" boundary included: 1) the Bering Strait with a given transport rate of the barotropic current and values of temperature and salinity; 2) river inflow areas, where the flow rate, zero salinity and temperature, equal to the temperature of the adjacent oceanic area were also set; 3) the southern boundary at 20° S, where water outflow was set, summarized water transport through the Bering Strait and riverine influx. The conditions at this boundary allow free advection outside the simulated area when the velocity is directed out of the area. If the velocity at the boundary is directed towards the region, then the climatic distribution data were used.

2.2. Experimental design. Boundary conditions in the Bering Strait

NCEP/NCAR reanalysis data [29], including surface air temperature, humidity, sea level pressure, precipitation intensity, downstream longwave and shortwave radiation fluxes, and wind speed in the surface layer, are used to form ocean and sea ice surface fluxes. The results for 2000 from previous calculations carried out since 1948 [30] were used as the initial distribution for oceanic and ice fields.

In this paper, the assessment of the contribution of the indicated changes in the heat input through the Bering Strait to the change in the state of waters and sea ice in the Chukchi and Beaufort Seas is based on numerical experiments performed for the period 2000–2019. using three types of boundary values. Figure 1 shows the used values of near-bottom and sea surface temperatures and volume transport in the Bering Strait. The conducted numerical experiments are presented in Table 1.

In the first experiment, further BS-20 (Bering Strait, 20 century), the Bering Strait climatology recommended in [31] for regional Arctic Ocean modeling was used as boundary conditions in the Bering Strait for the entire simulation period 2000–2019. Monthly values of water volume transport, near-bottom temperature and salinity, averaged over the time period 1990–2004, were obtained [31] from the processing of measurements at a depth of 45 m approximately 35 km north of the Bering Strait. The work [31] notes that the results of measurements in the surface layer are available in small quantities, and the available data indicate that the flow is homogeneous in winter. In summer, it was assumed that in the surface layer the temperature is higher than the bottom one by 1–2 °C. In the numerical experiment, the incoming flow was homogeneous. On the graph (Fig. 1), the values of water temperature and volume transport from this array are represented by a black line.

In [18], in connection with the changed characteristics of the waters entering through the Bering Strait, it was recommended to use new boundary conditions in numerical experiments simulating the period 2003–2015. The Bering Strait inflow rate in the new data was higher by 0.23 Sv, the average annual temperature was higher

Table 1

Numerical experiments information

Experiment code	Boundary conditions in the Bering Strait	Initial conditions	Simulation period
BS-20	Climate data 1990–2004 [31]	Estimated oceanic and ice fields for 2000 [30]	2000–2019
BS-21	2000–2003 — climate data [31], 2004–2019 — climate data [18]	Estimated oceanic and ice fields for 2000 [30]	2000–2019
BS obs	Measurement data for 2016–2019 [19, 32]	Estimated ocean and ice fields BS-21 for 2016	2016–2019

by 0.35 °C, the maximum deviation in the new data reached 5 °C. This array was used in the second experiment, then BS-21 (Bering Strait, 21 century) as the boundary conditions for the simulation period 2004–2019. For the period 2000–2003 the boundary conditions in experiment BS-21 were identical to experiment BS-20. On the graph (Fig. 1), data on near-bottom and sea surface temperatures and volume transport from this array are represented by a blue line.

The recommended values of oceanic characteristics in the Bering Strait [31, 18] are the averaging of measurement data over a long period of time and they do not reflect short-term fluctuations in the state of incoming Pacific waters. Analyzing daily observational data [32] in the Bering Strait, we prepared monthly average values of sea surface temperature, which reflected the processes of anomalous warming of the waters of the northern Pacific Ocean in 2016–2019, known as marine heat waves [33]. These surface temperature data with new measurements of near-bottom temperature and the Bering Strait volume transport [19], were used as boundary conditions for the third BS-obs numerical experiment. On the graph (Fig. 1), these data are represented by lines of red and yellow shades. These data generally exceed the climatic values used in BS-20 and BS-21.

3. Results

3.1. Results of numerical simulation. Climatic boundary conditions in the Bering Strait

As a result of numerical experiments based on the ice-ocean model, the fields of oceanic and ice characteristics are obtained. Two numerical experiments BS-20 and BS-21, which differ in the monthly average values of the characteristics of the Pacific waters, were carried out in the same period 2000–2019. The current field of the upper layer of the ocean, obtained as a result of these numerical experiments (Fig. 2), shows the transfer of water from the Bering Strait to the shelf of the Chukchi Sea. Propagating further into the deep part of the ocean, they are included in the water circulation system of a predominantly anticyclonic type, which has been characteristic of the present period since the early 2000s.

The average monthly values of the calculated fields make it possible to reveal the seasonal and interannual variability of the region's waters. Figure 3 shows the average monthly temperature fields at the selected horizons of 10, 50, and 100 m in certain periods of 2012–2013. Based on the presented distribution, it is possible to trace the transfer of warm waters formed on the shelf of the Chukchi Sea in summer to deep-water areas, in particular, to the Beaufort Sea.

Top panel in Figure 3 shows the average monthly temperature fields obtained for September 2012. The waters heated during the summer period are concentrated in the upper 50-m layer on the shelf of the Chukchi Sea, the maximum values are concentrated in the surface layer and the area where the Alaska current passes. Autumn-winter cooling of the surface layer (figure for December 2012, 10 m) is accompanied by intense mixing and heat transfer to the bottom layer of the shelf zone. The temperature distribution at depths of 50 and 100 m for December 2012 shows an expansion of the area occupied by positive values and heat propagation along the continental slope due to slope convection, the parameterization of which is included in the oceanic model [24]. Further propagation of the warm signal at depths of 100–150 m is due to water circulation. In the temperature field at a depth of 100 m for April 2013, Figure 3 shows a trend toward heat transfer to the Beaufort Sea. The situation in 2012–2013, shown in Fig. 2 is not an isolated case. The spreading of warm waters along the continental slope is also shown in the vertical section (Fig. 4).

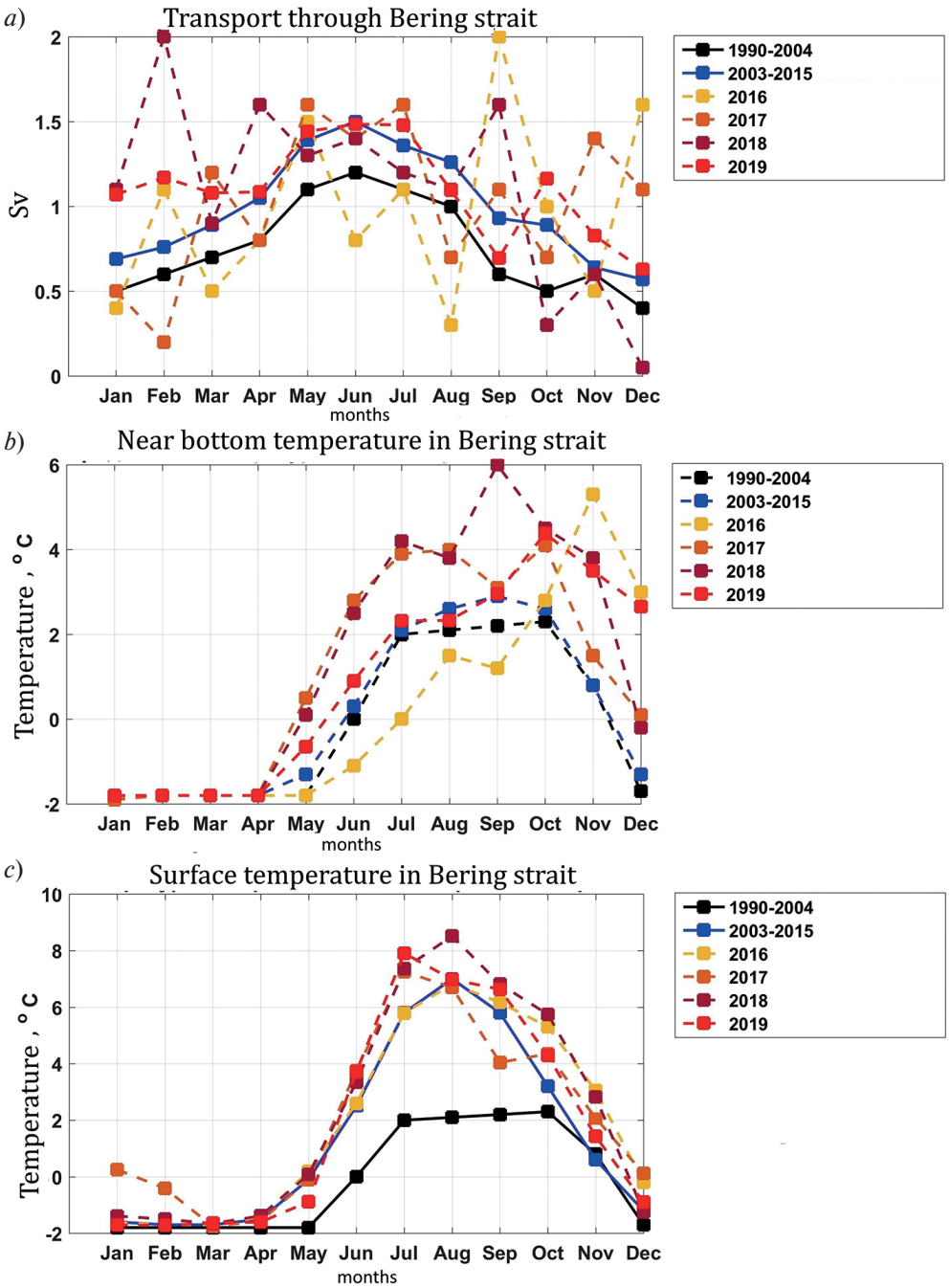

Fig. 1. Volume transport (*a*), bottom (*b*) and surface (*c*) temperature in the Bering Strait used in numerical simulations. The graph is based on data published in works [31, 18, 19, 32]

Figure 5, *a* shows graphs of seasonal temperature variability in the surface and near-bottom layers at one of the points in the area where heat is transferred from the shelf regions to the deep-water part. The graphs highlight the maximum values in the surface layer in the summer of 2007 and 2012, which corresponds to the minimum values of Arctic ice extent recorded based on observational data. The change in temperature in the near-bottom layer confirms the above conclusion about the heat transfer in the autumn-winter period from the adjacent regions. In the last calculation period timeseries show an increase in the amplitude of seasonal fluctuations in the temperature of the surface layer and a significant increase in temperature at a depth of 100 m.

To analyze the contribution of Pacific waters to the temperature increase in the intermediate layer of the deep part of the Chukchi Sea and the Beaufort Sea, we compared the results of BS-21 with the results of the

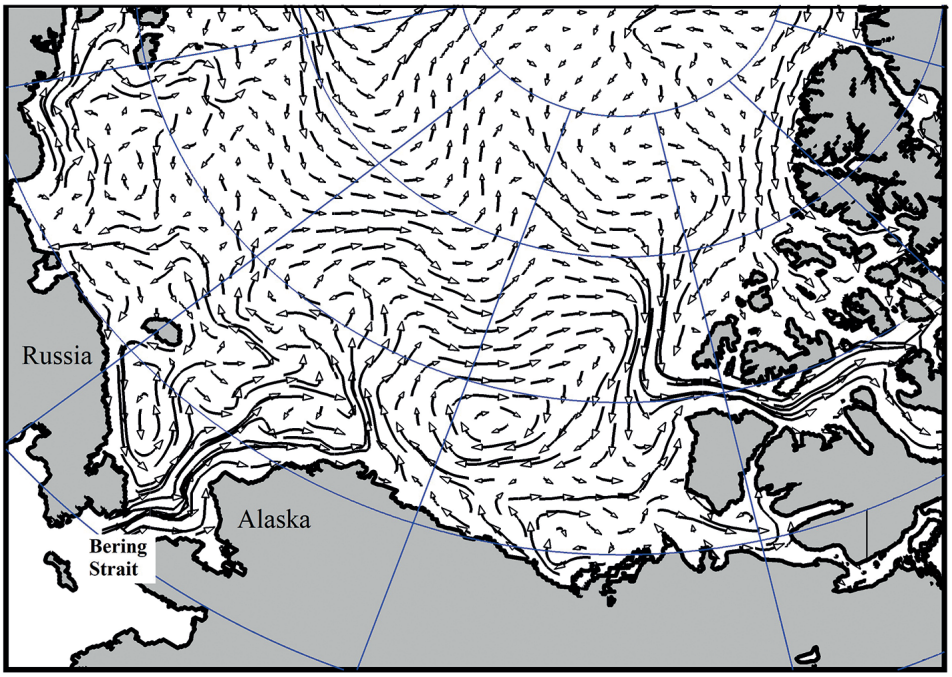

Fig. 2. 10-meter surface layer summer velocity obtained as a result of numerical experiments

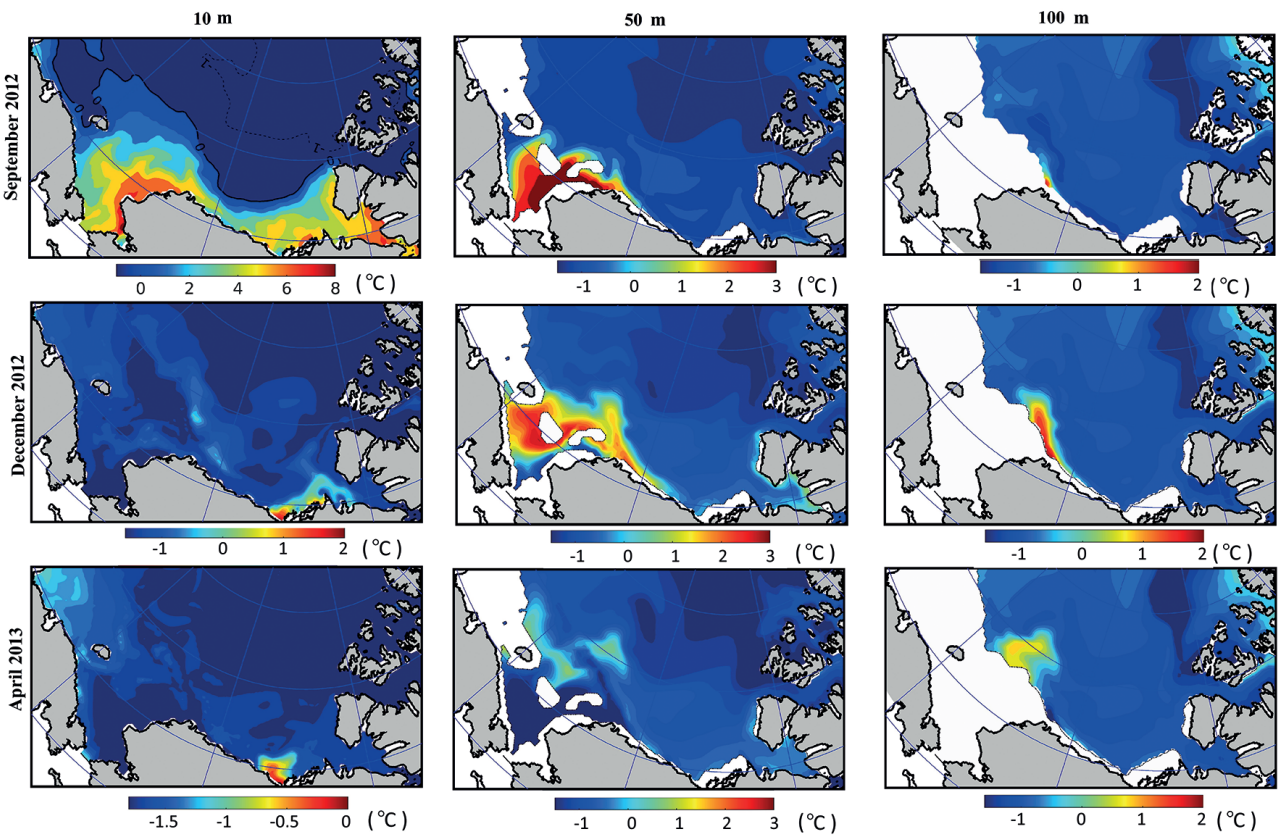

Fig. 3. Model temperature (°C) at the depths of 10 m, 50 m, and 100 m of the Chukchi and Beaufort Seas for September, December 2012, and April 2013. Result of the experiment BS-21

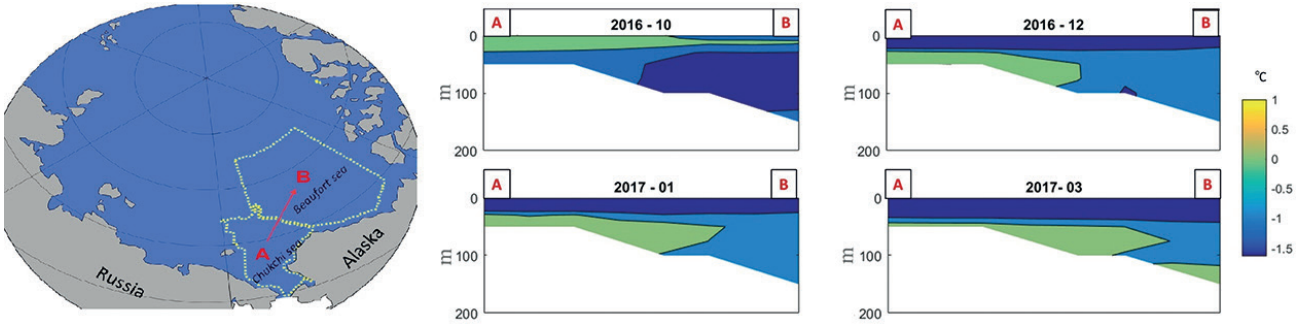

Fig. 4. Temperature at vertical section AB. The spreading of warm waters along the continental slope from October 2016 to March 2017 in numerical experiment BS-21

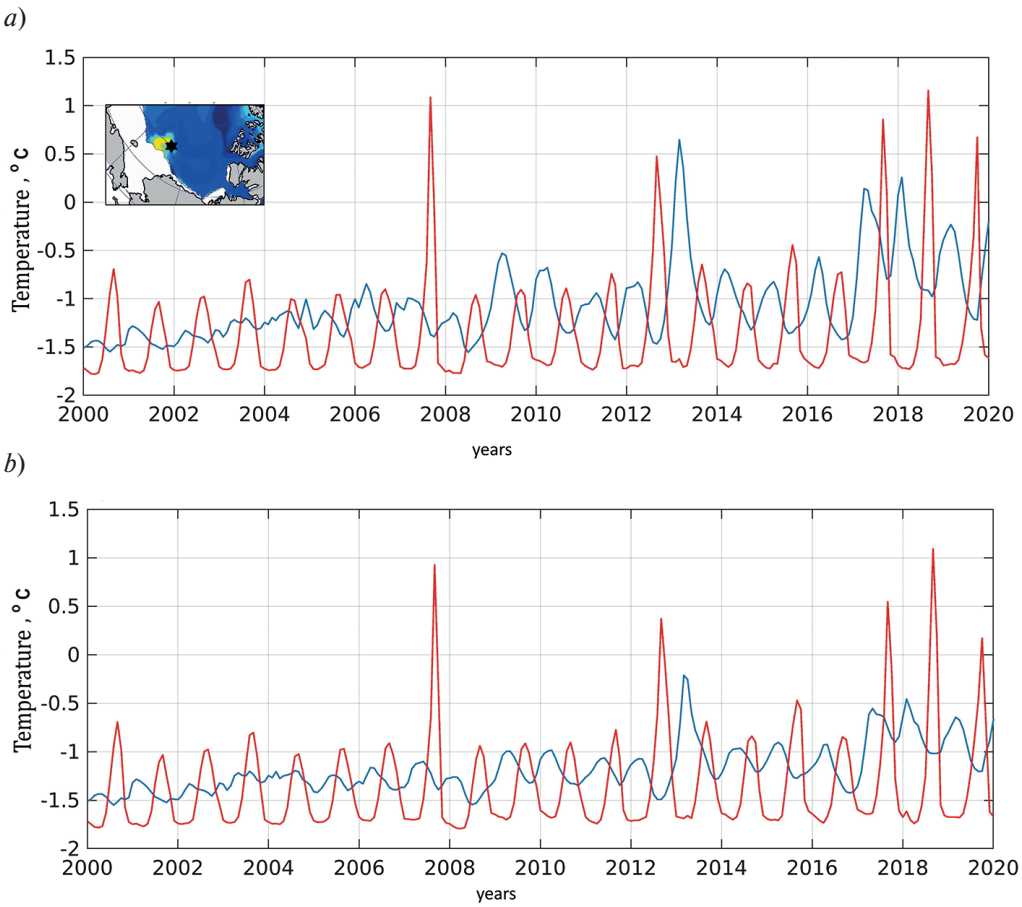

Fig. 5. Change in surface temperature (red line) and temperature in 100 m (blue line) at the point indicated by a black asterisk on the inset *a* — in the BS-21 experiment, *b* — in the BS-20 experiment

BS-20 numerical experiment, where values from the previously recommended climatology, acceptable until 2003, were used in the Bering Strait [31]. The seasonal course and interannual temperature variability at the previously identified point are shown in Fig. 5, *b*. A comparison of graphs for two experiments showed that in the BS-21 experiment, taking into account the new climatology, the water temperature values are higher than in the BS-20 experiment. Moreover, compared to the variability in the surface layer, the temperature change at a selected point at a depth of 100 m was more sensitive to changes in hydrological characteristics in the Bering Strait.

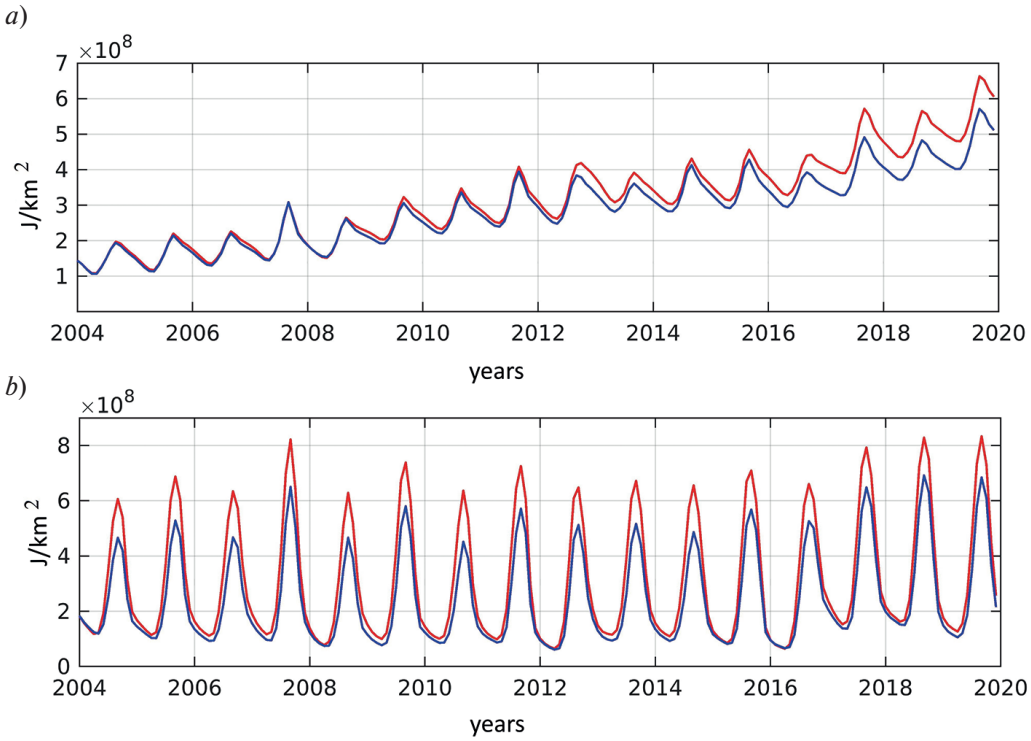

Fig. 6. Average heat content change (J/km^2) in the upper 150m layer in the Beaufort Sea (*a*) and the Chukchi Sea (*b*) based on the results of experiments BS-20, BS-21. The red line corresponds to the results of the BS-21 experiment, the blue line — BS-20

An assessment of the change in the heat content of water per unit area in the Beaufort and Chukchi Seas over the simulated period was carried out based on vertical integration over depth in the upper 150-meter layer of the potential temperature deviation from the freezing point

$$Q = \int_0^{\min(h(x,y),150)} \rho c_p \left(T - T_{ref}\right) dz. \quad (1)$$

Here c_p = 3996 J / (kg K) — specific heat of sea water, ρ = 1025 kg/m^3 — average density of sea water, T — water temperature, T_{ref} — freezing point, determined taking into account the salinity of sea water. Timeseries of heat content for the BS-20 and BS-21 experiments (Fig. 6) show that in addition to the heat input to the ocean due to summer heating and the reduction in the thickness and area of sea ice, the effect of a more intense input of Pacific waters leads to an increase in heat content in the Chukchi Sea and the Beaufort Sea.

The difference in heat content between experiments increased with time, in 2004 it was 10^7 J/km^2 and by 2019 reached the value 10^8 J/km^2. In the Chukchi Sea, seasonal fluctuations in heat content were more pronounced and appeared already in the first years of the calculation. In summer, the heat content values in the BS-21 experiment increased by an average of $1.2 \cdot 10^8$ J/km^2 compared to the BS-20 investigation. The proximity to the Bering Strait contributes to early ice melting, later freezing, as a result of which the number of ice-free days increases and solar radiation is absorbed, which in turn further increases the heat content in summer. In winter, the heat content drops sharply, there is no trend in heat accumulation, which is typical for the Beaufort Sea. In the last three years of calculation, an increase in both summer and winter values is noticeable.

3.2. Analysis of the heat flux entering the Bering Strait in numerical experiments

The values of temperature and volume transport water discharge used in numerical experiments make it possible to determine the heat flux entering through the Bering Strait $F_{B.}$

$$F_B = \rho \cdot c_p \cdot v_T \cdot \left(T - T_{ref}\right). \quad (2)$$

In addition to the notation for formula (1), here we use the notation v_T (m^3/s) volume transport through the strait. Fig. 7 shows graphs of time variability of monthly heat flux values in the period 2016–2019 for three experiments. Time averaging over 4 years showed that when using Bering Strait climatology [18] in experiment BS-21, the heat flux arrived on average more by $1.7 \cdot 10^{20}$ J/year than in the BS-20 experiment (Fig. 7).

A similar calculation showed that for the experiment BS-obs, on average, the increase in heat flux through the Bering Strait will be $1.257 \cdot 10^{20}$ J/year compared to BS-21 (Fig. 7). To assess the possible effect of the heat received during the year on the ice cover, we consider the relation

$$Q = \rho_{ice} \cdot S \cdot h \cdot c, \quad (3)$$

where $Q = 1.25 \cdot 10^{20}$ j, $\rho_{ice} = 918$ kg/m^3 — sea ice density $c = 332$ kJ/kg — specific heat of melting ice, S — ice cover area, h — ice thickness. Assuming an ice thickness of one meter, we got the ice cover area $S = 4.1 \cdot 10^5$ km^2. For comparison, in 1996 the ice cover in the Arctic was ~ $8 \cdot 10^6$ km^2, and in the anomalously warm year 2012 — ~ $3 \cdot 10^6$ km^2 [34]. Consequently, the additional heat that entered the Arctic Ocean through the Bering Strait in 2016–2019 is capable of melting a 1 m thick ice cover, commensurate with 1/7 of its area in the Arctic Ocean within the boundaries of 2012.

3.3. Impact of changes in the Bering Strait on ice cover. Comparison of the results of experiments BS-20 and BS-21

The change in the heat content of the waters is reflected in the state of the ice cover in the region under consideration. Numerical simulation results reflect a downward trend in the average annual sea ice volume for the Beaufort Sea and for the Chukchi Sea throughout the entire period 2004–2019 in the results of both experiments BS-20 and BS-21 (Fig. 8). A slight reduction in ice volume was obtained in BS-21 compared to BS-20. The relative difference in ice volume values for BS-21 compared to BS-20 was up to 4% for the Beaufort Sea. In the Chukchi Sea, the differences were more noticeable, and this value reaches 12% in 2017.

Differences in the position of the ice edge, determined by 25% ice concentration for BS-20 and BS-21, are shown in fig. 9 for the five months of 2019. The presented fields show less ice coverage for BS-21. The main changes were in the Chukchi Sea and in that part of the Beaufort Sea that borders the Chukchi Sea. It is here that the waters of the Bering Strait have a greater influence on the ice cover. It should be noted that despite the obtained response in the state of the ice cover in the BS-21 experiment, the results of the model fields did not result in a delay in the formation of the ice cover in the Bering Strait and the adjacent water area of the Chukchi Sea, known from observational data [34].

3.4. Boundary conditions in the Bering Strait in 2016–2019. Experiment BS -obs

Previous experiments used monthly climatology in the Bering Strait. It was obtained above that the additional heat flux calculated based on the difference in climatic conditions and average monthly values for

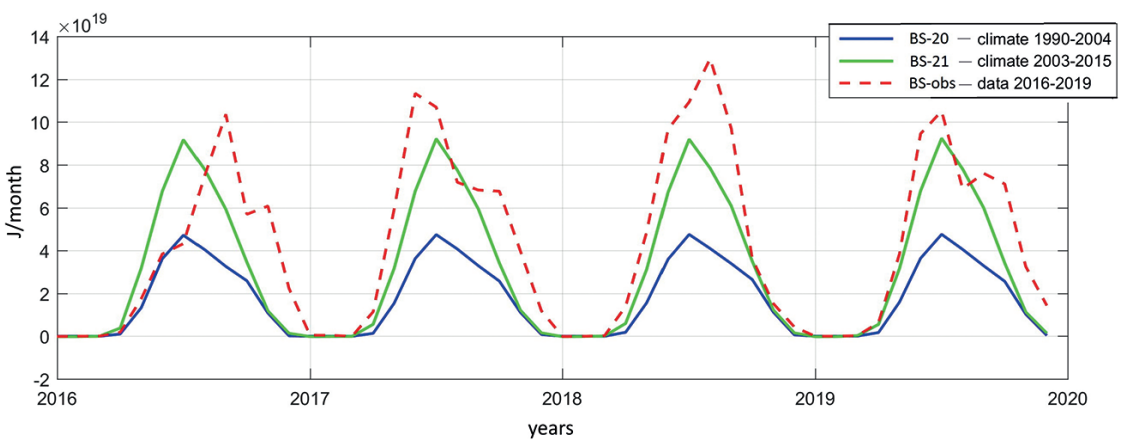

Fig. 7. Change in heat flux entering through the Bering Strait in the BS-20, BS-21, and BS-obs experiments

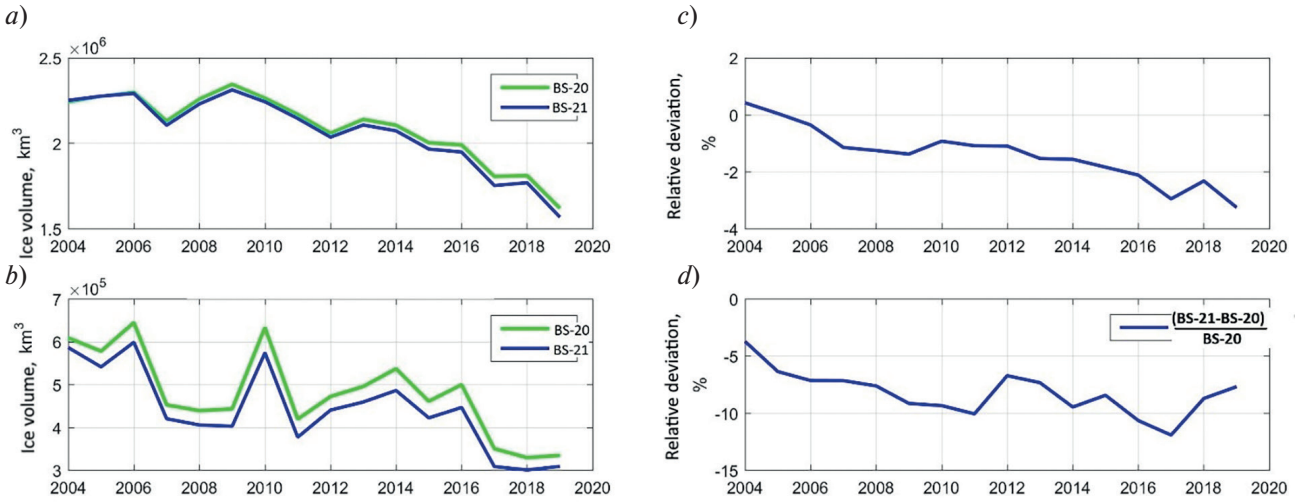

Fig. 8. Annual ice volume for the results of experiments BS-20, BS-21: *a* — in the Beaufort Sea; *b* — and the Chukchi Sea; deviation of ice volume for BS-21 from BS-20 $\frac{V_{BS-21}-V_{BS-20}}{V_{BS-20}}$; *c* — in the Beaufort Sea; *d* — in the Chukchi Sea

2016–2019 can melt a significant amount of ice. It is obvious that not all of the heat supplied will be used to melt the ice. The purpose of the Bs-obs numerical experiment was to study the sensitivity of model to the inflow of anomalously warm water through the Bering Strait for several years, which are taken into account in the model in the form of values of oceanological characteristics obtained from observational data [19, 32].

In the measurement data of 2016–2019 [19, 32] the temperature of incoming waters was generally higher than in the climate data used in BS-20 and BS-21 (Fig. 1). The exception was 2016: when the temperature in the Bering Strait from May to September was below climatic values, and only by November-December began to exceed them, the excess was 4–5 °C. During 2017–2019 the tendency to exceed the climatic values of temperature was preserved. A comparison of the results of numerical experiments BS-21 and BS-obs for the Chukchi Sea showed that the change in the average annual ice volume for BS-obs and BS-21 was less pronounced than when comparing BS-21 with BS-20 and did not exceed 5 %. In certain periods, the difference increases, so in December 2016 the difference was 10 %, in December 2017–20 %, in December 2018–10 %, and in December 2019–12 %. The difference in the heat content of the seas in the BS-obs experiment was about 1 % compared to the BS-21 experiment.

Comparison of the spatial distribution of the obtained fields of ice concentration as shown in Figs. 10 demonstrates that in December 2017, in the BS-obs experiment, the area of the Bering Strait and the shallow part of the Chukchi Sea remained ice-free. This differs the obtained distribution from the BS-21 experiment and is more consistent with the observational data [34].

4. Discussion

Our previous numerical studies analyzed the variability of the circulation of water masses, the thermohaline structure of the waters and the ice cover of the Arctic Ocean as a response to changes in the state of the atmosphere. In works [30, 35, 36], the variability of the trajectory of Atlantic and Pacific's waters entering the Arctic Ocean, caused by variations in atmospheric dynamics, was studied, and the influence of Pacific and Atlantic waters on the distribution and thickness of Arctic ice was shown. In this study, the emphasis is on the analysis of the sensitivity of the numerical model to an increase in the volume transport and temperature of the Pacific waters entering the shelf of the Chukchi Sea, known from the analysis of observational data [31, 18, 32, 19].

Two numerical experiments carried out using climatic data in the Bering Strait, typical for 1990–2004 and 2003–2015 simulate the seasonal and interannual variability of oceanic and ice fields. The modeling results show that the system of surface currents contributes to the transfer of warm Pacific waters through the Chukchi Sea shelf in a northerly direction and to the Beaufort Sea shelf. Heat transfer to the continental slope occurs in

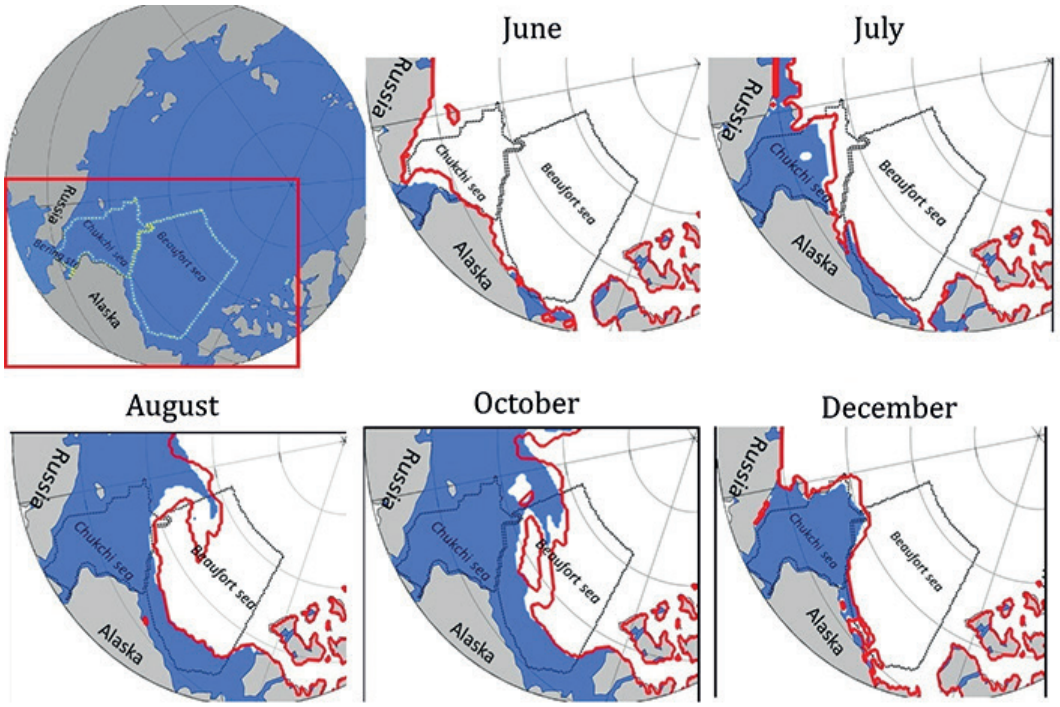

Fig. 9. Ice cover for several months of 2019 obtained from the BS-20 and BS-21 experiments. The distribution of ice cover for the results of the BS-20 experiment is shown in white. The red line shows the ice cover boundary for the results of the BS-21 experiment

the autumn-winter period along submarine canyons from adjacent regions and is reproduced within the grid resolution of the model and the parameterizations used, in particular, the parameterization of slope convection. This transfer is consistent with [10], from which it follows that the anticyclonic gyre of the Beaufort Sea and the generation of mesoscale eddies in the areas of submarine canyons weaken the cyclonic boundary current and contribute the movement of Pacific waters into the inner halocline of the Canadian Basin. In recent years, at the points located at the boundary of the shelf and deep-water areas, there is an increase in the amplitude of seasonal fluctuations in the temperature of the surface layer and a significant increase in temperature at a depth of 100 m. This process is typical for both experiments; however, at a depth of 100 m, the consequences of water temperature increase in the Bering Strait are pronounced.

In [20], the increase in heat content in the Beaufort Sea is attributed by the authors to anomalous solar heating of surface waters in the north of the Chukchi Sea due to the disappearance of the ice cover. Our results are consistent with this study. Changes in the heat content of the Chukchi Sea in numerical

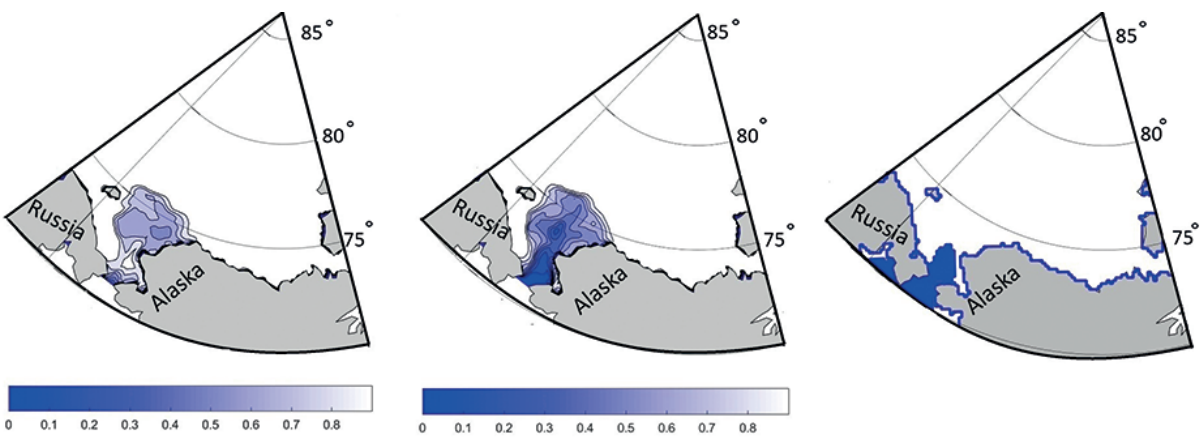

Fig. 10. Ice cover concentration for December 2017 obtained from the experiments BS-21 (left), BS-obs (center). Ice boundary for December 2017 according to NSIDC satellite observations [34] (right)

experiments show significant seasonal variations with an average amplitude $4 \cdot 10^8$ J/km^2 in the experiment with the Bering Strait climatology over period 1990–2004 [31] and $5.2 \cdot 10^8$ J/km^2 in the experiment used the boundary conditions data over period 2003–2015. The sensitivity of the heat content of waters to an increase in the incoming heat flux in the Bering Strait manifests itself in the first years of the calculation and is most pronounced in the summer season. In the last three years of calculation, the numerical model shows an increase in both summer and winter heat content values. In contrast to the Chukchi Sea, the change in the heat content of the upper 150 m layer of the Beaufort Sea shows a general upward trend since 2007. The consequences of an increase in the heat flux in the Bering Strait are manifested gradually with a pronounced cumulative effect both in the summer and winter seasons. The difference in heat content by 2019 reaches 10^8 J/km^2.

The general nature of the change in the water heat content and the sea ice volume in the study area in two experiments with the Bering Strait climatology shows that the changes occurring are caused by the Arctic atmosphere state. Nevertheless, as a result of the work it is shown that the Pacific waters entering the Arctic basin through the Bering Strait, and in 2003–2015 increased their temperature and volume transport compared to the period of 1990–2004, contribute to an increase in the heat content of the upper layer, as well as a reduction of the ice extent and volume in the Beaufort and Chukchi Seas. The main changes in ice concentration occur in the Chukchi Sea and in that part of the Beaufort Sea that borders the Chukchi Sea. It is here that the waters of the Bering Strait have a greater influence on the ice cover. The influence of changes in the characteristic of Pacific waters on the melting of sea ice in the Chukchi Sea is confirmed in the works [15–17] based on the analysis of observational data.

During the summer period 2016–2019 the northeastern part of the Pacific Ocean was characterized by an extremely warm state of the ocean, which led to the formation of an additional heat flux entering the Arctic Ocean through the Bering Strait and exceeding climatic values by an average of $1.25 \cdot 10^{20}$ J/year. Potentially, such a heat flux can melt a 1 m thick ice cover, commensurate with 1/7 of its area in the Arctic Ocean within the boundaries of 2012. According to estimates based on the analysis of observational data [19], the average annual heat flux through the Bering Strait is $3 - 6 \cdot 10^{20}$ J/year, which turns out to be comparable to the solar radiation flux in the Chukchi Sea and is capable of melting $1 - 2 \cdot 10^{20}$ km^2 of ice 1 m thick.

In our numerical experiment, carried out with these boundary data, the addition of an additional heat flux led to a later formation of ice in December and a reduction in the December volume of ice cover in the Chukchi Sea.

The disadvantage of the conducted research is the relatively coarse resolution of the numerical grid, which does not allow to simulate mesoscale eddies. The Rossby deformation radius in the Arctic varies depending on the region and reaches a maximum value of 15 km in the central part of the Canadian Basin [37]. On the continental slope of the Chukchi Sea, it varies from 5 to 8 km. This means that for a full-scale numerical simulation, it is necessary to use a finer grid resolution. For example, it was shown in [12] that mesoscale eddies on the continental slope of the Chukchi Sea are formed on a numerical grid of 2.5 km. It is assumed that on a finer grid, the response of the model to changing conditions in the Bering Strait will be greater, and the impact on the sea ice will increase due to more intense currents and heat transfer over longer distances.

5. Conclusion

Climatic changes in the Chukchi Sea and the Beaufort Sea were studied on the basis of numerical modeling using the SibCIOM regional ocean and sea ice model. Numerical experiments were carried out for the period 2000–2019 using the NCEP/NCAR reanalysis data that determine the fluxes on the surface of the ocean and sea ice, and the boundary conditions that specify the temperature, salinity, and volume transport of Pacific waters entering the Arctic Ocean through the Bering Strait. The influence of changes in the characteristics of the Pacific waters on the state of the ice cover and the heat content of the seas was studied based on a comparison of the results of three numerical experiments.

For their implementation in the Bering Strait, the following values of temperature, salinity, and water transport were set [31, 18, 19, 32]: a) monthly average climatic data over the period 1990–2004; b) monthly average climate data over the period 2003–2015; c) monthly average measurement data for the period 2016–2019. Climate data for the Bering Strait 2004–2015 differ from climate data for 1990–2004 increased values of water volume transport and temperature.

Based on the results of numerical experiments, we showed a general trend toward an increase in the heat content of waters and a decrease in the volume of ice in the Beaufort Sea and the Chukchi Sea in the period

from 2003–2019. This is primarily due to the state of the atmosphere in the Arctic region, but our results also show that the increase in temperature and volume transport of Pacific waters, which began after 2003, led to an additional increase in the heat content of the waters of both seas, a reduction in the area of sea ice and a delay in the timing of its formation in winter.

6. Funding

The work was carried out with the financial support of the RFBR, grant № 20-05-00536. The development of a numerical model of the ocean and sea ice is carried out within the framework of the state task of the ICM-MG SB RAS № 0251-2021-0003. The Siberian Branch of the Russian Academy of Sciences Siberian Supercomputer Center is gratefully acknowledged for providing supercomputer facilities.

References

1. *Nikiforov E.G.*, *Shpaikher A.O.* Regularities of formation of large-scale oscillations of hydrological regime of the Arctic Ocean. *Leningrad*, *Gidrometeoizdat,* 1980. 270 p. (in Russian).
2. *Shtokman V.B.* Influence of wind on the currents in the Bering Strait, the reasons for their high speeds and its prevailing northern direction. Critical review of modern ideas about currents in the Bering Strait and their causes. *Trudy IOAN USSR*. 1957, XXV, 171–197 (in Russian).
3. *Gudkovich Z.M.* On the nature of the Pacific current in Bering Strait and the causes of its seasonal variations. *Deep Sea Research*. 1962, 9, 507–510.
4. *Coachman L.K.*, *Aagaard K.* On the water exchange through Bering Strait. *Limnology and Oceanography*. 1966, 11, 44–59.
5. *Serreze M.C.*, *Barrett A.P.*, *Slater A.G.*, *Woodgate R.A.*, *Aagaard K.*, *Lammers R.B.*, *Steele M.*, *Moritz R.*, *Meredith M.*, *Lee C.M.* The large-scale freshwater cycle of the Arctic. *Journal of Geophysical Research*. 2006, 111, C11010. doi:10.1029/2005JC003424
6. *Coachman L.K.*, *Aagaard K.*, *Tripp R.B.* Bering Strait: The regional physical oceanography / *Seattle*, *WA*: *University of Washington Press*, 1975. 172 p.
7. *Steele M.*, *Morison J.*, *Ermold W.*, *Rigor I.*, *Ortmeyer M.* Circulation of summer Pacific halocline water in the Arctic Ocean. *Journal of Geophysical Research*. 2004, 109, C02027. doi:10.1029/2003JC002009
8. *Aagaard K.*, *Coachman L.*, *Carmack E.* On the halocline of the Arctic Ocean. *Deep-Sea Research Part I*. 1981, 28, 529–545. doi:10.1016/0198-0149(81)90115-1
9. *Woodgate R.A.*, *Aagaard K.*, *Weingartner T.J.* A year in the physical oceanography of the Chukchi Sea: Moored measurements from autumn 1990–1991. *Deep-Sea Research Part II*. 2005, 52 (24–26), 3116–3149. doi:10.1016/j.dsr2.2005.10.016
10. *Pickart R.S.*, *Weingartner J.T.*, *Pratt L.J.*, *Zimmermann S.*, *Torres D.J.* Flow of winter-transformed Pacific water into the Western Arctic. *Deep-Sea Research*. 2005, 52, 3175–3198. doi:10.1016/J.DSR2.2005.10.009
11. *Spall M.A.*, *Pickart R.S.*, *Fratantoni P.*, *Plueddemann A.* Western Arctic shelfbreak eddies: Formation and transport. *Journal of Physical Oceanography*. 2008, 38, 1644–1668. doi:10.1175/2007JPO3829.1
12. *Watanabe E.*, *Hasumi H. Pa*cific Water transport in the western Arctic Ocean simulated by an eddy-resolving coupled sea ice–ocean model. *Journal of Physical Oceanography*. 2009, 39, 2194–2211. doi:10.1175/2009JPO4010.1
13. *Timmermans M.-L.*, *Proshutinsky A.*, *Golubeva E.*, *Jackson J.*, *Krishfield R.*, *McCall M.*, *Platov G.*, *Toole J.*, *Williams W.* Mechanisms of Pacific Summer Water variability in the Arctic's Central Canada Basin. *Journal of Geophysical Research*: *Oceans*. 2014, 119, 111, 7523–7548. doi:10.1002/2014JC010273
14. *MacKinnon J.A.*, *Simmons H.L.*, *Hargrove J.* et al. A warm jet in a cold ocean. *Nature Communications*. 2021, 12, 2418. doi:10.1038/s41467-021-22505-5
15. *Spall M.A.* Circulation and water mass transformation in a model of the Chukchi Sea. *Journal of Geophysical Research*. 2007, 112, C05025. doi:10.1029/2005jc003364
16. *Woodgate R.*, *Stafford K.*, *Prahl F.* A Synthesis of Year-Round Interdisciplinary Mooring Measurements in the Bering Strait (1990–2014) and the RUSALCA Years (2004–2011). *Oceanography*. 2015, 28, 46–67. doi:10.5670/oceanog.2015.57
17. *Serreze M.C.*, *Crawford A.D.*, *Stroeve J.*, *Barrett A.P.*, *Woodgate R.A.* Variability, trends, and predictability of seasonal sea ice retreat and advance in the Chukchi Sea. *Journal of Geophysical Research*: *Ocean*. 2016, 121, 10, 7308–7325. doi:10.1002/2016jc011977
18. *Woodgate R.* Increases in the Pacific inflow to the Arctic from 1990 to 2015, and insights into seasonal trends and driving mechanisms from year-round Bering Strait mooring data. *Progress in Oceanography*. 2017, 160, 124–154. doi:10.1016/j.pocean.2017.12.007

19. *Woodgate R.*, *Peralta Ferriz C.* Warming and Freshening of the Pacific Inflow to the Arctic From 1990–2019 Implying Dramatic Shoaling in Pacific Winter Water Ventilation of the Arctic Water Column. *Geophysical Research Letters*. 2021, 48, 9, e2021GL092528. doi:10.1029/2021GL092528
20. *Timmermans M–L.*, *Toole J.*, *Krishfield R.* Warming of the interior Arctic Ocean linked to sea ice losses at the basin margins. *Science Advances*. 2018, 4, 8. doi:10.1126/sciadv.aat6773
21. *Golubeva E.*, *Platov G.* On improving the simulation of Atlantic Water circulation in the Arctic Ocean. *Journal of Geophysical Research*: *Oceans*. 2007, 112, C4. doi:10.1029/2006JC003734
22. *Golubeva E.N.* Numerical modeling of the Atlantic Water circulation in the Arctic Ocean using QUICKEST scheme. *Vychislitel'nye Tekhnologii*. 2008, 13, 5, 11–24 (in Russian).
23. *Leonard B.P.* A stable and accurate convective modeling procedure based on quadratic upstream interpolation. *Computer Methods in Applied Mechanics and Engineering*. 1979, 19, 59–98.
24. *Leonard B.P.*, *Lock A.P.*, *MacVean M.K.* Conservative explicit unrestricted-timestep multidimensional constancy-preserving advection schemes. *Monthly Weather Review*. 1996, 124, 2588–2606. doi:10.1175/1520-0493(1996)124<2588: CEUTSM>2.0.CO;2
25. *Golubeva E.N.*, *Ivanov Ju.A.*, *Kuzin V.I.*, *Platov G.A.* Numerical modeling of the World Ocean circulation including upper ocean mixed layer. *Oceanology*. 1992, 32, 3, 395–405 (in Russian).
26. *Platov G.A.* Numerical modeling of the Arctic Ocean deepwater formation: Part II. Results of regional and global experiments. *Izvestiya*, *Atmospheric and Oceanic Physics*. 2011, 47, 377–392. doi:10.1134/S0001433811020083
27. *Hunke E.C.*, *Dukowicz J.K.* An elastic-viscous-plastic model for ice dynamics. // Journal of Physical Oceanography. 1997, 27, 1849–1867. doi:10.1175/1520–0485(1997)027<1849: AEVPMF>2.0.CO;2
28. *Murray R.J.* Explicit generation of orthogonal grids for ocean models. *Journal of Computational Physics*. 1996, 126, 251–273.
29. *Kalnay E.*, *Kanamitsu M.*, *Kistler R.*, *Collins W.*, *Deaven D.*, *Gandin L.*, *Iredell M.*, *Saha S.*, *White G.*, *Woollen J.* et al. The NCEP/NCAR40-Year Reanalysis Project. *Bulletin of the American Meteorological Society*. 1996, 77, 437–471. 2.0.CO;2., NCEP/NCAR Global Reanalysis Products, 1948-continuing, Research Data Archive URL: https://psl.noaa.gov/data/gridded/data.ncep.reanalysis.html (18.03.2022).
30. *Golubeva E.N.*, *Platov G.A.*, *Iakshina D.F.* Numerical simulations of the current state of waters and sea ice in the Arctic Ocean. *Led i Sneg*. 2015, 2 (130), 81–92 (in Russian). doi:10.15356/2076-6734-2015-2-81-92
31. *Woodgate R.*, *Aagaard K.* Monthly temperature, salinity, and transport variability of the Bering Strait through flow. *Geophysical Research Letters*. 2005, 32, 4. doi:10.1029/2004GL021880
32. *Reynolds R.W.*, *Smith T.M.*, *Liu C.*, *Chelton D.B.*, *Casey K.S.*, *Schlax M.G.* Daily High-Resolution Blended Analyses for Sea Surface Temperature. *Journal of Climate*. 2007, 20, 5473–5496. NOAA high resolution SST data are provided by NOAA/OAR/ESRL PSD (Boulder, CO, USA) from their website URL: https://psl.noaa.gov/data/gridded/data.noaa.oisst.v2.highres.html (18.03.2022).
33. *Carvalho K.S.*, *Smith T.E.*, *Wang S.* Bering Sea marine heatwaves: Patterns, trends and connections with the Arctic. *Journal of Hydrology*. 2021, 600, 126462. doi:10.1016/j.jhydrol.2021.126462
34. National Snow and Ice Data Center. URL: https://nsidc.org (18.03.2022).
35. *Golubeva E.N., Platov G.A.* Numerical modeling of the Arctic Ocean ice system response to variations in the atmospheric circulation from 1948 to 2007. Izvestiya, Atmospheric and Oceanic Physics. 2009, 45, 1, 137–151. doi:10.1134/S0001433809010095
36. *Aksenov Y.*, *Karcher M.*, *Proshutinsky A.*, *Gerdes R.*, *de Cuevas B.*, *Golubeva E.*, *Kauker F.*, *Nguyen A.T.*, *Platov G.A.*, *Wadley M.* et al. Arctic pathways of Pacific Water: Arctic Ocean Model Intercomparison experiments. *Journal of Geophysical Research*: *Oceans*. 2016, 121, 27–59. doi:10.1002/2015JC011299
37. *Nurser A.J.G.*, *Bacon S.* The Rossby radius in the Arctic Ocean. *Ocean Science*. 2014, 10, 967–975. doi:10.5194/os-10-967-2014

Литература

1. *Никифоров Е.Г.*, *Шпайхер А.О.* Закономерности формирования крупномасштабных колебаний гидрологического режима Северного Ледовитого океана. Л.: Гидрометеоиздат, 1980. 270 с.
2. *Штокман В.Б.* Влияние ветра на течения в Беринговом проливе, причины их больших скоростей и преобладающего его северного направления. Критический обзор современных представлений о течениях в Беринговом проливе и об их причинах // Труды ИО АН СССР. 1957. Т. XXV. С. 171–197.
3. *Gudkovich Z.M.* On the nature of the Pacific current in Bering Strait and the causes of its seasonal variations // Deep Sea Research. 1962. Vol. 9. P. 507–510.
4. *Coachman L.K.*, *Aagaard K.* On the water exchange through Bering Strait // Limnology and Oceanography. 1966. № 11. P. 44–59.

5. *Serreze M.C.*, *Barrett A.P.*, *Slater A.G.*, *Woodgate R.A.*, *Aagaard K.*, *Lammers R.B.*, *Steele M.*, *Moritz R.*, *Meredith M.*, *Lee C.M.* The large-scale freshwater cycle of the Arctic // Journal of Geophysical Research. 2006. 111. C11010. doi:10.1029/2005JC003424
6. *Coachman L.K.*, *Aagaard K.*, *Tripp R.B.* Bering Strait: The regional physical oceanography / Seattle, WA: University of Washington Press, 1975. 172 p.
7. *Steele M.*, *Morison J.*, *Ermold W.*, *Rigor I.*, *Ortmeyer M.*, *Shimada K.* Circulation of summer Pacific halocline water in the Arctic Ocean // Journal of Geophysical Research. 2004. 109, C02027. doi:10.1029/2003JC002009
8. *Aagaard K.*, *Coachman L.*, *Carmack E.* On the halocline of the Arctic Ocean // Deep-Sea Research Part I. 1981. Vol. 28, N 6. P. 529–545. doi:10.1016/0198-0149(81)90115-1
9. *Woodgate R.A.*, *Aagaard K.*, *Weingartner T.J.* A year in the physical oceanography of the Chukchi Sea: Moored measurements from autumn 1990–1991 // Deep-Sea Research Part II. 2005. Vol. 52 (24–26). P. 3116–3149. doi:10.1016/j.dsr2.2005.10.016
10. *Pickart R.S.*, *Weingartner J.T.*, *Pratt L.J.*, *Zimmermann S.*, *Torres D.J.* Flow of winter-transformed Pacific water into the Western Arctic // Deep-Sea Research. 2005. Vol. 52. P. 3175–3198. doi:10.1016/J.DSR2.2005.10.009
11. *Spall M.A.*, *Pickart R.S.*, *Fratantoni P.*, *Plueddemann A.* Western Arctic shelfbreak eddies: Formation and transport // Journal of Physical Oceanography. 2008. 38. P. 1644–1668. doi:10.1175/2007JPO3829.1
12. *Watanabe E.*, *Hasumi H.* Pacific Water transport in the western Arctic Ocean simulated by an eddy-resolving coupled sea ice–ocean model // Journal of Physical Oceanography. 2009. Vol. 39. P. 2194–2211. doi:10.1175/2009JPO4010.1
13. *Timmermans M.-L.*, *Proshutinsky A.*, *Golubeva E.*, *Jackson J.*, *Krishfield R.*, *McCall M.*, *Platov G.*, *Toole J.*, *Williams W.* Mechanisms of Pacific Summer Water variability in the Arctic's Central Canada Basin // Journal of Geophysical Research: Oceans. 2014. Vol. 119, N 111. P. 7523–7548. doi:10.1002/2014JC010273
14. *MacKinnon J.A.*, *Simmons H.L.*, *Hargrove J.* et al. A warm jet in a cold ocean // Nature Communications. 2021. Vol. 12. 2418. doi:10.1038/s41467-021-22505-5
15. *Spall M.A.* Circulation and water mass transformation in a model of the Chukchi Sea // Journal of Geophysical Research. 2007. Vol. 112. C05025. doi:10.1029/2005jc003364
16. *Woodgate R.*, *Stafford K.*, *Prahl F.* A Synthesis of Year-Round Interdisciplinary Mooring Measurements in the Bering Strait (1990–2014) and the RUSALCA Years (2004–2011) // Oceanography. 2015. Vol. 28. P. 46–67. doi:10.5670/oceanog.2015.57
17. *Serreze M.C.*, *Crawford A.D.*, *Stroeve J.*, *Barrett A.P.*, *Woodgate R.A.* Variability, trends, and predictability of seasonal sea ice retreat and advance in the Chukchi Sea // Journal of Geophysical Research: Ocean. 2016. Vol. 121, N 10. P. 7308–7325. doi:10.1002/2016jc011977
18. *Woodgate R.* Increases in the Pacific inflow to the Arctic from 1990 to 2015, and insights into seasonal trends and driving mechanisms from year-round Bering Strait mooring data // Progress in Oceanography. 2017. Vol. 160. P. 124–154. doi:10.1016/j.pocean.2017.12.007
19. *Woodgate R., Peralta Ferriz C.* Warming and Freshening of the Pacific Inflow to the Arctic from 1990–2019 Implying Dramatic Shoaling in Pacific Winter Water Ventilation of the Arctic Water Column // Geophysical Research Letters. 2021. Vol. 48, N 9. e2021GL092528. doi:10.1029/2021GL092528
20. *Timmermans M–L.*, *Toole J.*, *Krishfield R.* Warming of the interior Arctic Ocean linked to sea ice losses at the basin margins // Science Advances. 2018. Vol. 4, N 8. doi:10.1126/sciadv.aat6773
21. *Golubeva E.*, *Platov G.* On improving the simulation of Atlantic Water circulation in the Arctic Ocean // Journal of Geophysical Research: Oceans. 2007. Vol. 112, N C4. doi:10.1029/2006JC003734
22. *Голубева Е.Н.* Численное моделирование динамики Атлантических вод в Арктическом бассейне с использованием схемы QUICKEST // Вычислительные технологии. 2008. Т. 13, № 5. С. 11–24.
23. *Leonard B.P.* A stable and accurate convective modeling procedure based on quadratic upstream interpolation // Computer Methods in Applied Mechanics and Engineering. 1979. V. 19. P. 59–98.
24. *Leonard B.P.*, *Lock A.P.*, *MacVean M.K.* Conservative explicit unrestricted-timestep multidimensional constancy-preserving advection schemes // Monthly Weather Review. 1996. Vol. 124. P. 2588–2606. doi:10.1175/1520–0493(1996)124<2588: CEUTSM>2.0.CO;2
25. *Голубева Е.Н.*, *Иванов Ю.А.*, *Кузин В.И.*, *Платов Г.А.* Численное моделирование циркуляции Мирового океана с учетом верхнего квазиоднородного слоя. // Океанология. 1992. Т. 32, № 3. С. 395–405.
26. *Платов Г.А.* Численное моделирование формирования глубинных вод Северного Ледовитого океана. Часть II: Результаты региональных и глобальных расчетов // Известия РАН. Физика атмосферы и океана. 2011. Т. 47, № 3. С. 409–425.
27. *Hunke E.C.*, *Dukowicz J.K.* An elastic-viscous-plastic model for ice dynamics // Journal of Physical Oceanography. 1997. Vol. 27. P. 1849–1867. doi:10.1175/1520–0485(1997)027<1849: AEVPMF>2.0.CO;2
28. *Murray R.J.* Explicit generation of orthogonal grids for ocean models // Journal of Computational Physics. 1996. Vol. 126. P. 251–273.

29. *Kalnay E.*, *Kanamitsu M.*, *Kistler R.*, *Collins W.*, *Deaven D.*, *Gandin L.*, *Iredell M.*, *Saha S.*, *White G.*, *Woollen J.* et al. The NCEP/NCAR40-Year Reanalysis Project // Bulletin of the American Meteorological Society. 1996. Vol. 77. P. 437–471. 2.0.CO;2., NCEP/NCAR Global Reanalysis Products, 1948-continuing, Research Data Archive URL: https://psl.noaa.gov/data/gridded/data.ncep.reanalysis.html (дата обращения: 18.03.2022).
30. *Голубева Е.Н.*, *Платов Г.А.*, *Якшина Д.Ф.* Численное моделирование современного состояния вод и морского льда Северного Ледовитого океана // Лёд и Снег. 2015. № 2 (130). С. 81–92. doi:10.15356/2076-6734-2015-2-81-92
31. *Woodgate R.*, *Aagaard K.* Monthly temperature, salinity, and transport variability of the Bering Strait through flow // Geophysical Research Letters. 2005. Vol. 32, N4. doi:10.1029/2004GL021880
32. *Reynolds R.W.*, *Smith T.M.*, *Liu C.*, *Chelton D.B.*, *Casey K.S.*, *Schlax M.G.* Daily High-Resolution Blended Analyses for Sea Surface Temperature // Journal of Climate. 2007. Vol. 20. P. 5473–5496. NOAA high resolution SST data are provided by NOAA/OAR/ESRL PSD (Boulder, CO, USA) from their website URL: https://psl.noaa.gov/data/gridded/data.noaa.oisst.v2.highres.html (дата обращения: 18.03.2022).
33. *Carvalho K.S.*, *Smith T.E.*, *Wang S.* Bering Sea marine heatwaves: Patterns, trends and connections with the Arctic // Journal of Hydrology. 2021. Vol. 600. 126462. doi:10.1016/j.jhydrol.2021.126462
34. National Snow and Ice Data Center. URL: https://nsidc.org (дата обращения: 18.03.2022).
35. *Голубева Е.Н.*, *Платов Г.А.* Численное моделирование отклика Арктической системы океан-лед на вариации атмосферной циркуляции 1948–2007 гг. // Известия РАН, Физика атмосферы и океана. 2009. Т. 45, № 1. С. 145–160.
36. *Aksenov Y.*, *Karcher M.*, *Proshutinsky A.*, *Gerdes R.*, *de Cuevas B.*, *Golubeva E.*, *Kauker F.*, *Nguyen A.T.*, *Platov G.A.*, *Wadley M.* et al. Arctic pathways of Pacific Water: Arctic Ocean Model Intercomparison experiments. // Journal of Geophysical Research: Oceans. 2016. Vol. 121. P. 27–59. doi:10.1002/2015JC011299
37. *Nurser A.J.G.*, *Bacon S.* The Rossby radius in the Arctic Ocean // Ocean Science. 2014. Vol. 10. P. 967–975. doi:10.5194/os-10-967-2014